Improving the Numerical Solution of Soil Moisture–Based Richards Equation for Land Models with a Deep or Shallow Water Table

XUBIN ZENG AND MARK DECKER

Department of Atmospheric Sciences, The University of Arizona, Tucson, Arizona

(Manuscript received 22 January 2008, in final form 1 July 2008)

ABSTRACT

The soil moisture–based Richards equation is widely used in land models for weather and climate studies, but its numerical solution using the mass-conservative scheme in the Community Land Model is found to be deficient when the water table is within the model domain. Furthermore, these deficiencies cannot be reduced by using a smaller grid spacing. The numerical errors are much smaller when the water table is below the model domain. These deficiencies were overlooked in the past, most likely because of the more dominant influence of the free drainage bottom boundary condition used by many land models. They are fixed here by explicitly subtracting the hydrostatic equilibrium soil moisture distribution from the Richards equation. This equilibrium distribution can be derived at each time step from a constant hydraulic (i.e., capillary plus gravitational) potential above the water table, representing a steady-state solution of the Richards equation. Furthermore, because the free drainage condition has serious deficiencies, a new bottom boundary condition based on the equilibrium soil moisture distribution at each time step is proposed that also provides an effective and direct coupling between groundwater and surface water.

1. Introduction

The vertical movement of soil moisture (θ) is governed by the Richards equation derived from θ conservation (Richards 1931). This partial differential equation for θ [rather than the soil matric potential (Ψ)] is solved numerically with gravitational drainage as the bottom boundary condition in many land models (Dickinson et al. 1993; Sellers et al. 1996; Mitchell et al. 2004). The accuracy of these numerical solutions is crucial not only to the terrestrial water cycle but also to the energy cycle (Dickinson et al. 2006), nitrogen and carbon cycles (Thornton and Zimmermann 2007; Bonan and Levis 2006), and global change (Cox et al. 2000).

In general, numerical solutions contain truncation errors that usually depend on the grid spacing in land models (typically from a few centimeters near surface to more than one meter for deep soil layers). The motivation for raising the issue of truncation errors comes from the well-known fact about the vertical momentum equation in the atmosphere (Holton 2004). This equation is dominated by the approximate hydrostatic balance between the pressure gradient force and the gravitational force, and the hydrostatic pressure is not directly involved in the vertical movement of air parcels. If the original form of the vertical momentum equation is used directly for numerical solutions, the typical (and finite) grid spacing in atmospheric models would result in large truncation errors in the computation of vertical velocity—even though these errors do converge to zero as the grid spacing and time step approach zero. To solve this problem, the vertical momentum equation with the hydrostatic pressure subtracted, rather than its original form, is used for numerical solutions in atmospheric models (Holton 2004).

Similar to the above atmospheric equation, the hydrostatic equilibrium soil moisture distribution, derived under the assumption of constant hydraulic—that is, capillary (or matric) plus gravitational—potential above water table, represents a steady-state solution of the (differential) Richards equation. Therefore, the following question, as the counterpart of the above atmospheric equation, is asked: If the current form of the θ-based Richards equation is directly used for numerical solutions, how do the truncation errors affect the computation of the vertical movement of θ in land models?

Corresponding author address: Xubin Zeng, Department of Atmospheric Sciences, The University of Arizona, P.O. Box 210081, Tucson, AZ 85721.
E-mail: xubin@atmo.arizona.edu

DOI: 10.1175/2008JHM1011.1

A related issue is the treatment of saturated layers within a land model domain—that is, a shallow water table. Theoretically, because (saturated) soil moisture does not change but the matric potential still changes in the saturated layers (Celia et al. 1990; Pan and Wierenga 1995; Ross 2003), numerical solutions of the θ-based Richards equation are not appropriate for simulating water fluxes in soils with saturated regions. In practice, however, the same θ-based Richards equation has been used in land models over arid regions (with a deep water table) and the tropical rain forests (with a shallow water table). The question is then, how large are the errors of the numerical solutions when the land model domain contains saturated layers?

The purpose of this paper is to demonstrate that the direct use of the θ-based Richards equation to saturated layers and, to a lesser degree, unsaturated layers would generate significant numerical errors in the θ computation, and both problems can be fixed by explicitly subtracting the hydrostatic equilibrium soil moisture distribution from the θ-based Richards equation. The importance of the hydrostatic equilibrium state in the soil was also recognized before (Koster et al. 2000) in which the soil water transfer between the surface and the root zone (or between the root zone and the water table) is proportional to the surface layer (or root zone) soil moisture deviation from the equilibrium state. The relation of our work to previous efforts on the Richards equation with Ψ as the dependent variable as used in groundwater hydrology and soil physics (e.g., Celia et al. 1990) will also be discussed later. Other issues related to the Richards equation (e.g., the subgrid horizontal variability; Famiglietti and Wood 1994; Albertson and Montaldo 2003) are out of the scope of this study and will not be addressed here.

An obvious question related to these two issues—the truncation errors with a shallow or deep water table—is, why were these issues overlooked in the past by the land modeling community, at least for weather and climate studies? This is most probably related to the bottom boundary condition, which has a significant influence on the simulation of θ distribution but cannot be determined accurately in regional and global studies. In other words, deficiencies of the bottom boundary condition may be even more serious than the above issues and hence may mask the deficiencies of the numerical solution itself with a deep or shallow water table. For this reason, a new bottom boundary condition will also be proposed in this paper. Section 2 quantifies deficiencies related to the numerical solutions and the bottom boundary condition, whereas section 3 discusses our solutions. Section 4 provides the summary and further discussions.

2. The original θ-based Richards equation

a. Formulations

For one-dimensional vertical water flow in soils, the conservation of mass (i.e., the Richards equation) is

$$\frac{\partial \theta}{\partial t} = \frac{\partial}{\partial z}\left[K\frac{\partial(\Psi + z)}{\partial z}\right] - S, \tag{1}$$

where θ is the volumetric soil water content, t is time, z is height above the data in the soil column (positive upward), S is a soil moisture sink term (e.g., transpiration loss in the rooting zone), which was not included in the original equation (Richards 1931), K is the hydraulic conductivity, Ψ is the soil matric (or capillary) potential, and z, as used in the hydraulic potential ($\Psi + z$), also represents the gravitational potential. Note that other components of the total soil water potential [e.g., osmotic (or solute) potential, pneumatic (air or vapor) potential, and chemical potential] are not considered in (1).

The soil water flux q as used in (1) is called the Darcy's law:

$$q = -K\frac{\partial(\Psi + z)}{\partial z}, \tag{2}$$

and the top boundary condition at the soil surface (z_0) for (1) is

$$q_0 = P + M - E_g - R_g, \tag{3}$$

where P is the rainfall reaching the soil surface, M is the snowmelt, E_g is ground evaporation, and R_g is surface runoff. In general, E_g and R_g are dependent on θ in land models (e.g., Oleson et al. 2004). At the bottom of a land model domain (z_b), the gravitational drainage condition is used in many land models (Dickinson et al. 1993; Sellers et al. 1996; Oleson et al. 2004; Mitchell et al. 2004):

$$q_b = K(z_b), \tag{4}$$

which is obtained by setting $\partial\Psi/\partial z = 0$ in (2). In fact, it was mentioned in Lohmann et al. (1998) that 13 of the 16 land models in their model intercomparison used (4) or a combination of (4) with other considerations (e.g., topography and bedrocks). Many land models for weather and climate studies also use the formulations for K and Ψ (Clapp and Hornberger 1978):

$$K = K_{\text{sat}}(\theta/\theta_{\text{sat}})^{2B+3}; \quad \Psi = \Psi_{\text{sat}}(\theta/\theta_{\text{sat}})^{-B}, \tag{5}$$

where the saturated hydraulic conductivity K_{sat} and saturated matric potential Ψ_{sat} are exponential functions of the percentage of sand, the saturated soil moisture content (or porosity) θ_{sat} is a linear function of the

percentage of sand, and the exponent B is a linear function of the percentage of clay (Cosby et al. 1984). Sensitivity tests using the Brooks and Corey (1964) relation will also be reported later.

Equations (1) and (2) can be solved numerically using a mass-conservative scheme,

$$(z_{i-1/2} - z_{i+1/2})\left(\overline{\theta_i}^{n+1} - \overline{\theta_i}^{n}\right)/\Delta t = -q_{i-1/2}^{n+1} + q_{i+1/2}^{n+1} - \overline{S_i}, \tag{6}$$

where Δt is the time interval (typically from a few minutes to one hour) between time step n and $n + 1$, $\overline{\theta_i}$ and $\overline{S_i}$ are layer-averaged quantities between $z_{i+1/2}$ and $z_{i-1/2}$, and $q_{i-1/2}$ and $q_{i+1/2}$ represent fluxes at layer interfaces. Their expressions from the Community Land Model, version 3 (CLM3; Oleson et al. 2004), are used here. Furthermore, the 10 soil layer structures with model bottom at 3.44-m depth from the CLM3 are used in most of the numerical simulations, although different soil layers are also used in sensitivity tests. For all numerical tests, we use soil texture with 40% sand and 40% clay (and hence 20% silt), independent of soil depth, so that $\theta_{\text{sat}} = 0.44$ (mm^3 of water per mm^3 of soil), $K_{\text{sat}} = 0.0038$ (mm s^{-1}), $B = 9.3$, and $\Psi_{\text{sat}} = -227.0$ (mm).

b. *Truncation errors of the numerical solution (6) when the water table is below the land model domain*

Mathematically, the soil moisture distribution $\theta_E(z)$ is derived from a constant hydraulic potential (C) above the water table:

$$\Psi_E + z = \Psi_{\text{sat}}[\theta_E(z)/\theta_{\text{sat}}]^{-B} + z = C, \tag{7}$$

which represents a steady-state solution (or hydrostatic equilibrium state, denoted by the subscript E) of (1) because $q \equiv 0$ from (2) and $\partial\theta_E/\partial t \equiv 0$ from (1) (omitting the source/sink term). It is a special case of the general steady-state solution derived from a constant q (to be discussed later). When $\theta_E(z)$ is applied to the numerical scheme (6), the layer-averaged θ and Ψ are computed as

$$\overline{\theta_i} = \int_{z_{i-1/2}}^{z_{i+1/2}} \frac{\theta_E(z)\,dz}{(z_{i+1/2} - z_{i-1/2})} \quad \text{and} \quad \overline{\Psi_i} = \Psi_{\text{sat}}\left(\frac{\overline{\theta_i}}{\theta_{\text{sat}}}\right)^{-B}. \tag{8}$$

Using (7), $\overline{\theta_i}$ in (8) can then be analytically obtained as

$$\overline{\theta_i} = \frac{\theta_{\text{sat}}(\Psi_{\text{sat}})^{1/B}[(C - z_{i-1/2})^{1-1/B} - (C - z_{i+1/2})^{1-1/B}]}{(z_{i+1/2} - z_{i-1/2})(1 - 1/B)}. \tag{9}$$

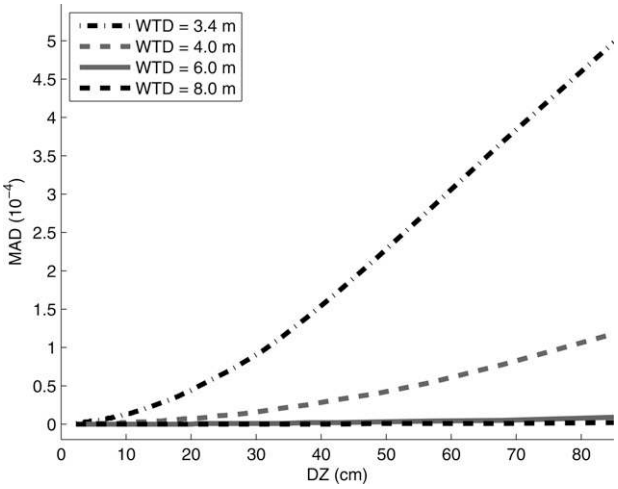

FIG. 1. The dependence of MAD between θ after 30 days of integration and its initial equilibrium state on uniform grid spacing (Δz) and the initial WTD, all at or below the bottom of the model domain. Zero fluxes are used as the top and bottom boundary conditions in all simulations.

Although Ψ_E is a linear function of z in (7), $\overline{\Psi_i}$ computed from (8) and (9) is a nonlinear function of z. As the grid spacing—that is, $z_{i+1/2} - z_{i-1/2}$—approaches zero, it is straightforward to demonstrate using (8) and (9) that $\overline{\theta_i}$ and $\overline{\Psi_i}$ would correctly converge to θ_E and Ψ_E, respectively. For a typical grid spacing of a few centimeters near the surface to more than one meter for deep soil layers (as used in land models for weather and climate studies), however, $\overline{\Psi_i}$ deviates from Ψ_E, so that the flux q in (2) is also a function of z and $\overline{\theta_i}$, and would change with time in (6). To quantify the effect of these truncation errors on the maintenance of an initial hydrostatic equilibrium soil moisture distribution $\theta_E(z)$, we assume the same soil texture as provided at the end of section 2a, omit the sink term S in (1), and assume $q_0 = 0$ in (3)—that is, zero flux at the top. Furthermore, we assume zero flux at the bottom (i.e., $q_b = 0$). Then (6) is integrated from an initial equilibrium state, which is obtained using three steps: 1) prescribing an initial water table depth (WTD) of 4 m (or $z_w = -4$ m), 2) obtaining $C = \Psi_{\text{sat}} + z_w$ (see discussion in section 3), and 3) obtaining soil moisture for each layer from (9).

After 30 days of integration using the 10 soil layers in the CLM3 from an initial equilibrium state of θ, the θ distribution is found to approach its steady state. This final state is slightly different from the initial state, and the differences in soil moisture [or the truncation errors of the numerical scheme (6)] can be quantified by the mean absolute deviation (MAD) from all soil layers between θ after 30 days of integration and its initial equilibrium state. Figure 1 shows the dependence of MAD on the grid spacing (Δz) and the initial water

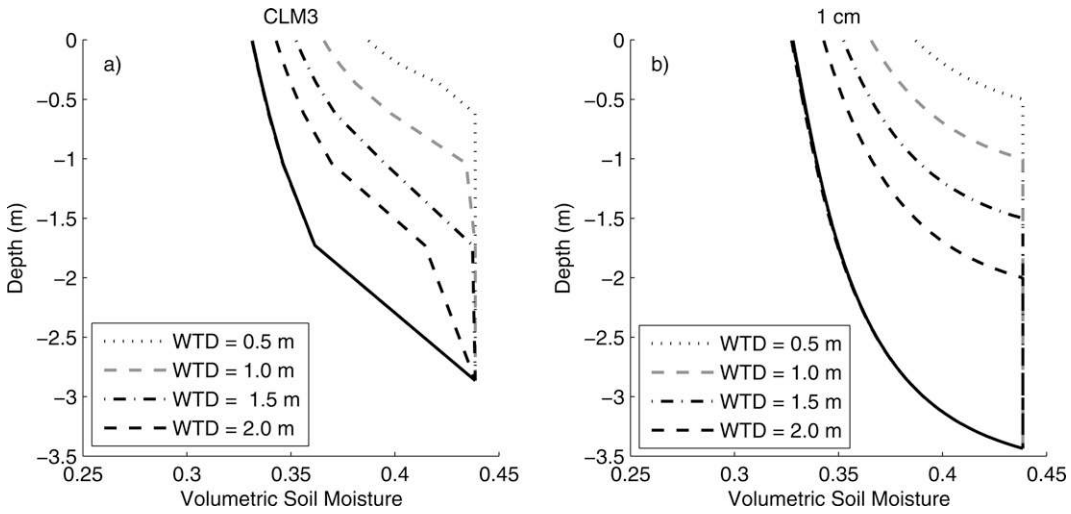

FIG. 2. (a) The initial equilibrium state of soil moisture (dotted, dashed, or dotted–dashed lines) and its distribution after 30 days of integration (solid lines) with different initial WTDs at 0.5, 1, 1.5, and 2 m using the 10 soil layers in the CLM3. All four solid lines overlap with each other. (b) Same as (a) except with a uniform grid spacing of 1 cm. Zero fluxes are used as the top and bottom boundary conditions in all simulations, and the extra soil water above saturation in each layer is removed as runoff at the end of each time step.

table depth z_w (all at or below the bottom of the model domain). For a deep water table depth of 8 m, MAD is very small, nearly independent of Δz. For a shallower water table depth of 3.4 m (at the bottom of the model domain), MAD increases nearly exponentially with Δz. Overall, however, the truncation errors are small when the water table is below the model domain.

c. *Deficiencies of the numerical solution (6) when the water table is within the land model domain*

As mentioned in section 1, numerical solutions of the θ-based Richards equation, theoretically, are not appropriate for simulating water fluxes in soils with saturated regions (e.g., Ross 2003). In practice, however, when saturated soil layers exist in the model domain, the same θ-based Eq. (1) is used in land models for weather and climate studies. The consequence is that some of these saturated layers become supersaturated, and the extra soil water above the saturation is usually removed as runoff in land models. Figure 2 shows the results with a different initial water table depth (all within the model domain) and different Δz. Note that even with the same initial distribution of $\theta(z)$, different layer thicknesses lead to different initial distribution of layer-averaged soil moisture [cf. (9)], as indicated by the dotted, dashed, and dotted–dashed lines in Fig. 2a versus Fig. 2b.

For all simulations in Fig. 2, saturated layers cannot be maintained, even though zero fluxes are used as the top and bottom boundary conditions. Furthermore, with the same Δz, the θ distribution after 30 days of integration would be the same (with the bottom layer saturated), independent of the initial water table depth (Figs. 2a or 2b). Comparing the small deviations in Fig. 1, the θ deviation after 30 days of integration from the initial equilibrium state in Fig. 2 is much larger (particularly near the water table depth) when the initial water table is within the model domain. In addition, these large deviations using 10 soil layers (Fig. 2a) cannot be reduced by using 344 layers with $\Delta z = 1$ cm (Fig. 2b), which is very different from the simulation when the water table is below the model domain (Fig. 1).

Therefore, based on results from Figs. 1 and 2, the answers to the first two questions raised in section 1 are as follows: 1) the numerical solution (6) of the θ-based Richards equation (1) is inappropriate for simulating water fluxes in soils with saturated regions (i.e., contains significant errors that cannot be reduced by using a smaller grid spacing), and 2) the numerical errors are much smaller when the water table is below the model domain.

d. *Deficiencies of the bottom boundary condition (4)*

An obvious question related to the above two issues is, why were these issues overlooked in the past by the land modeling community, at least for weather and climate studies? This is likely related to the deficiencies of the bottom boundary condition (4) as used in many land models. In other words, deficiencies of the bottom boundary condition may be even more serious than the

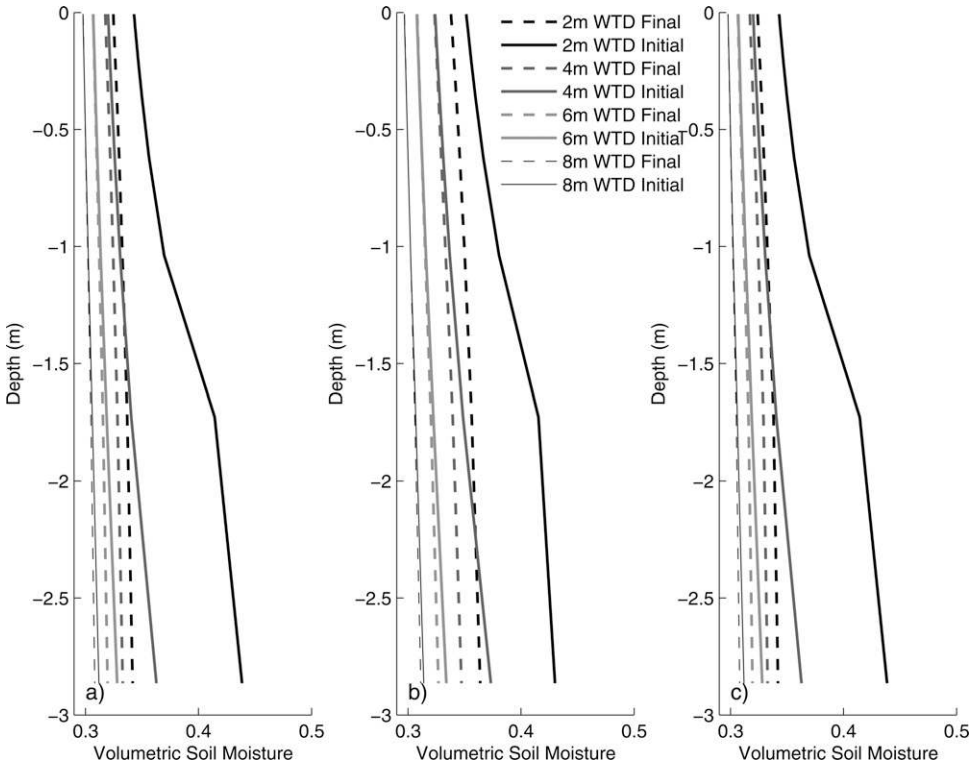

FIG. 3. (a) Soil moisture distribution at the initial equilibrium states with WTDs at 2, 4, 6, and 8 m, respectively, (solid lines) and after 30 days of integrations of (6) with zero flux as the top boundary condition and (4) as the bottom boundary condition (dashed lines). (b) Same as (a) except using the Brooks and Corey (1964) relation to replace the Clapp and Hornberger (1978) relation. (c) Same as (a) except using the modified form of the Richards equation (11) to replace (1).

above issues and hence may mask the deficiencies of the numerical solution itself, particularly when a shallow water table is present.

One deficiency of (4) is that soil water can only move down as a result of gravitational potential, and the state of soil water below the model domain (e.g., groundwater) cannot affect the soil water above.

Another deficiency of (4) is the requirement of an unrealistically high precipitation rate to maintain a relatively wet soil moisture at which vegetation can transpire without soil moisture stress. To illustrate this point, the steady state solution of (1) for a single soil layer can be obtained by integrating (1) along with (2)–(5):

$$q_0 - S_t = K(z_b) = K_{\text{sat}}(\theta/\theta_{\text{sat}})^{2B+3}, \qquad (10)$$

where S_t represents the total transpiration from the rooting zone. As an example, we take the soil texture provided at the end of section 2a and assume that vegetation can transpire without soil moisture stress at $\Psi_f = -0.15$ Pa (or -1.52×10^3 mm) or $\theta_f = 0.36$ based on (5). The minimum ($q_0 - S_t$) required to maintain θ_f can then be obtained from (10) as 4.3 mm day^{-1}. As a rough estimate, assuming evapotranspiration is 50% of the precipitation and surface runoff is 50% of the total runoff—that is, surface runoff and bottom drainage—then the minimum precipitation rate to maintain θ_f would be 17.2 mm day^{-1}, which is much greater than the precipitation rate even over most of the tropical rain forests. This implies that, with the use of (4), soil would be too dry nearly everywhere.

To evaluate the effect of (4) on the soil moisture simulations, we have repeated the simulations in Figs. 1 and 2 except with (4) as the bottom boundary condition. Compared with the case with a water table depth of 2 m in Fig. 2a, the deviations of θ after 30 days of integration from the initial state are much larger, particularly for bottom layers (Fig. 3a). These deviations become smaller with the increase of the initial water table depth from 2 to 8 m (Fig. 3a). In other words, the deficiency of (4) is most critical when the water table is relatively shallow.

The dependence of these results on the number of model layers (with the model bottom at 3.44-m depth) using (1) and (4) is shown in Fig. 4. After 30 days of

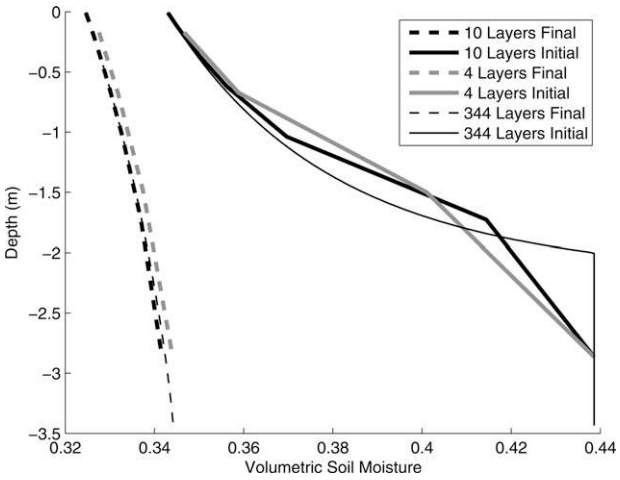

FIG. 4. Same as Fig. 3 except with a WTD of 2 m (solid lines). Results with 4, 10 (the control simulation), and 344 even layers ($\Delta z = 1$ cm) are shown.

integration, the soil moisture distributions become similar. In other words, the deficiencies of (4) are insensitive to the number of model layers and hence cannot be reduced by using finer vertical resolutions.

3. A modified form of the θ-based Richards equation

Section 2 has demonstrated the deficiencies of the numerical solution (6) and the free drainage bottom boundary condition (4), particularly under shallow water table conditions. The critical question is then, how can these deficiencies be removed or reduced?

The main idea of this study, as motivated by the form of the vertical momentum equation used by atmospheric models, is to subtract the equilibrium state (7) from (1), that is,

$$\begin{aligned}\partial(\Psi + z)/\partial z &= \partial(\Psi + z - C)/\partial z \\ &= \partial[\Psi + z - (\Psi_E + z)]/\partial z \\ &= \partial(\Psi - \Psi_E)/\partial z,\end{aligned}$$

and the modified form of the Richards equation becomes

$$\frac{\partial\theta}{\partial t} = \frac{\partial}{\partial z}\left[K\frac{\partial(\Psi - \Psi_E)}{\partial z}\right] - S. \tag{11}$$

To obtain $\theta_E(z)$ for use in (11), (7) is applied between the water table depth (z_w, with saturated soil) and height z:

$$\Psi_E + z = \Psi_{\text{sat}}[\theta_E(z)/\theta_{\text{sat}}]^{-B} + z = \Psi_{\text{sat}} + z_w \tag{12}$$

with the mass-conservation constraint of

$$\sum_{i=1}^{N}(\theta_{\text{sat}} - \overline{\theta_i})\Delta z_i = \int_{z_b}^{z_0}[\theta_{\text{sat}} - \theta_E(z)]\,dz, \tag{13}$$

where N is the number of soil layers, Δz_i is the layer thickness, and $\overline{\theta_i}$ is the average soil moisture in layer i. If z_w is specified (e.g., as an initial condition in most of the simulations here), $\theta_E(z)$ can be directly obtained from (12). If $\overline{\theta_i}$ (i = 1, N) is known—as an initial condition or during model integrations—the expression of $\theta_E(z)$ from (12) can be used to analytically solve the integral in (13) as a nonlinear function of z_w, which can then be solved iteratively to obtain z_w and hence $\theta_E(z)$. The same approach was widely used to compute z_w in the past (e.g., Chen and Kumar 2001).

We have repeated the simulations in Figs. 1 and 2 except (11) replaces (1) and found that the soil moisture distribution does not change with time—that is, the initial hydrostatic equilibrium state is maintained and hence no figures are shown—independent of the number of soil layers used or the initial water table depth (within or below the model domain). This demonstrates that our modified form of θ-based Richards equation (11) effectively removes the deficiencies of the numerical solution (6) with a deep or shallow water table.

When land models are used for weather and climate studies, zero flux is generally not a good bottom boundary condition because it assumes there are bedrocks at the bottom or that the soil water below the domain and in the bottom model layer are always in equilibrium—that is, satisfy the condition (12). Although the bottom condition (4) has serious deficiencies as discussed in section 2d, many land models still use it because few, if any, better alternatives are available for regional and global modeling studies.

To preliminarily address this difficult issue, we add an extra soil layer ($N + 1$) with the same thickness (Δz_N) as the bottom layer of a land model and compute $\overline{\theta_{N+1}}$ directly from $\theta_E(z)$ [cf. (9)]. Then the bottom condition becomes

$$q_b = K(z_b)\frac{\partial(\Psi - \Psi_E)}{\partial z}, \tag{14}$$

where the vertical gradient is computed using soil moisture in the bottom layer ($\overline{\theta_N}$) and in the extra layer ($\overline{\theta_{N+1}}$), just as between any adjacent layers in the model domain.

Note that there is no perfect bottom condition for regional or global applications. Equation (14) is generally better than the free drainage or zero flux condition because it allows for the direct (vertical) coupling of groundwater with unsaturated soil moisture in the

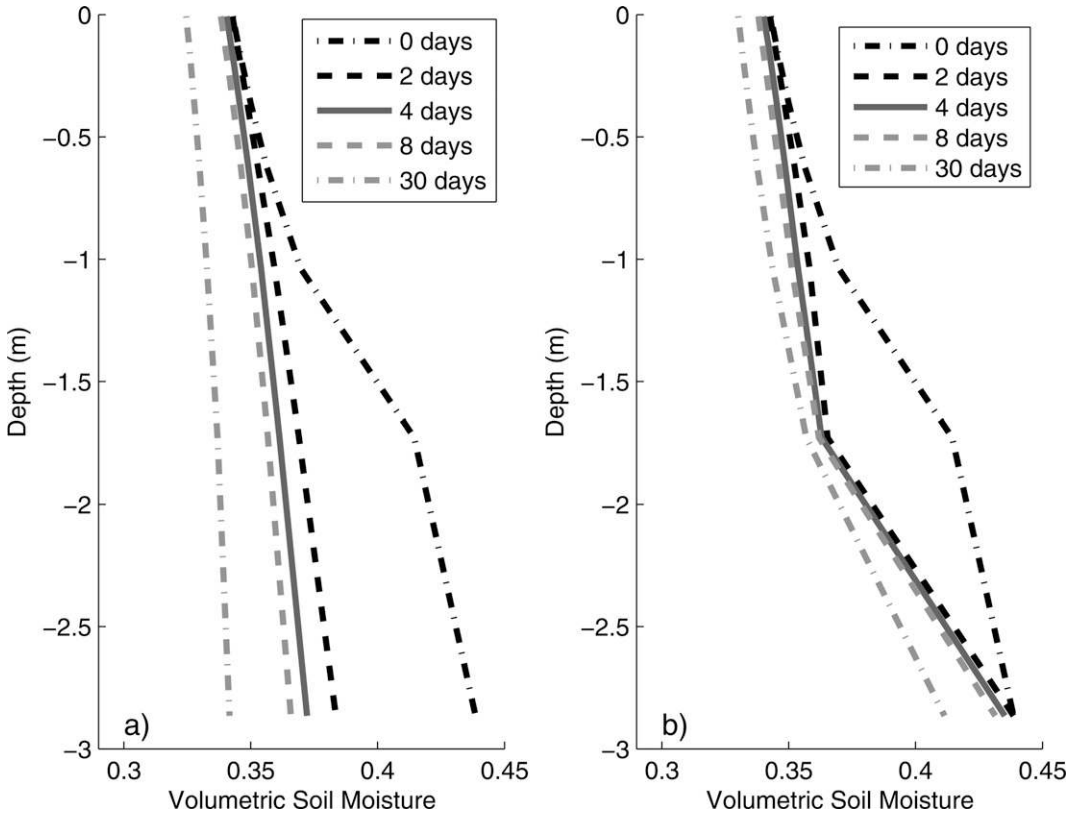

FIG. 5. The 30-day evolution of average soil moisture in 10 layers from an initial equilibrium state with an initial WTD of 2 m. (a) Integration of (6) using (1) with $S = q_0 = 0$ and bottom boundary condition (4). (b) Same as (a) except using the new bottom boundary condition (14) that itself does not destroy the equilibrium state.

model domain. This will be further discussed in section 4, and a more detailed discussion will be presented in a separate study (Decker and Zeng 2008, manuscript submitted to *J. Adv. Model. Earth Syst.,* hereafter DeZe). The uncertainty of (14) is related to the specific way $\overline{\theta_{N+1}}$ is computed—that is, simply based on the hydrostatic equilibrium state $\theta_E(z)$ at each time step in our approach.

We have repeated all the computations in Figs. 1–4 except using (11) and (14) to replace (1) and (4) (or the zero flux condition), respectively. It is found that the soil moisture distribution does not change with time—that is, the initial hydrostatic equilibrium state is maintained and hence no figures are shown. In other words, if the soil moisture distribution is in a hydrostatic equilibrium state, (14) is equivalent to the zero flux condition.

To separate the effects of the numerical solution (6) based on (1) or (11) versus the bottom boundary condition (4) or (14), we have performed simulations using all four combinations:

- (1) and (4) (i.e, control simulations, discussed in section 2);
- (11) and (14) (discussed above and further discussed below);
- (11) and (4) [to evaluate the effect of (11) alone]; and
- (1) and (14) [to evaluate the effect of (14) alone].

The comparison of Fig. 3a and 3c indicates that, if the free drainage condition (4) is applied, the use of (1) or (11) does not make a difference. This further demonstrates the dominating effect of the free drainage condition and may explain why the deficiencies of the numerical solution (6) of the θ-based Richards equation (1) were overlooked in the past by the land modeling community. Although (14) itself would not cause the deviation of θ from the initial equilibrium state, Fig. 5b shows that (1) still leads to the drop of θ and hence a nonzero flux at the bottom of the model domain. This suggests that (14) itself cannot remove the deficiencies of the numerical solution (6) of the Richards equation (1). On the other hand, (14) does reduce the deficiencies, as indicated by the slower rate of decrease of θ in Fig. 5b in comparison with that in Fig. 5a in which (1) and the free drainage condition (4) are used.

As an additional test, we evaluate (1) and (4) versus (11) and (14) with a constant surface flux $q_0 = -1$ mm day^{-1} (e.g., evaporation) or 1 mm day^{-1} (e.g., precipitation). Figure 6 shows that soil moisture after 30 days

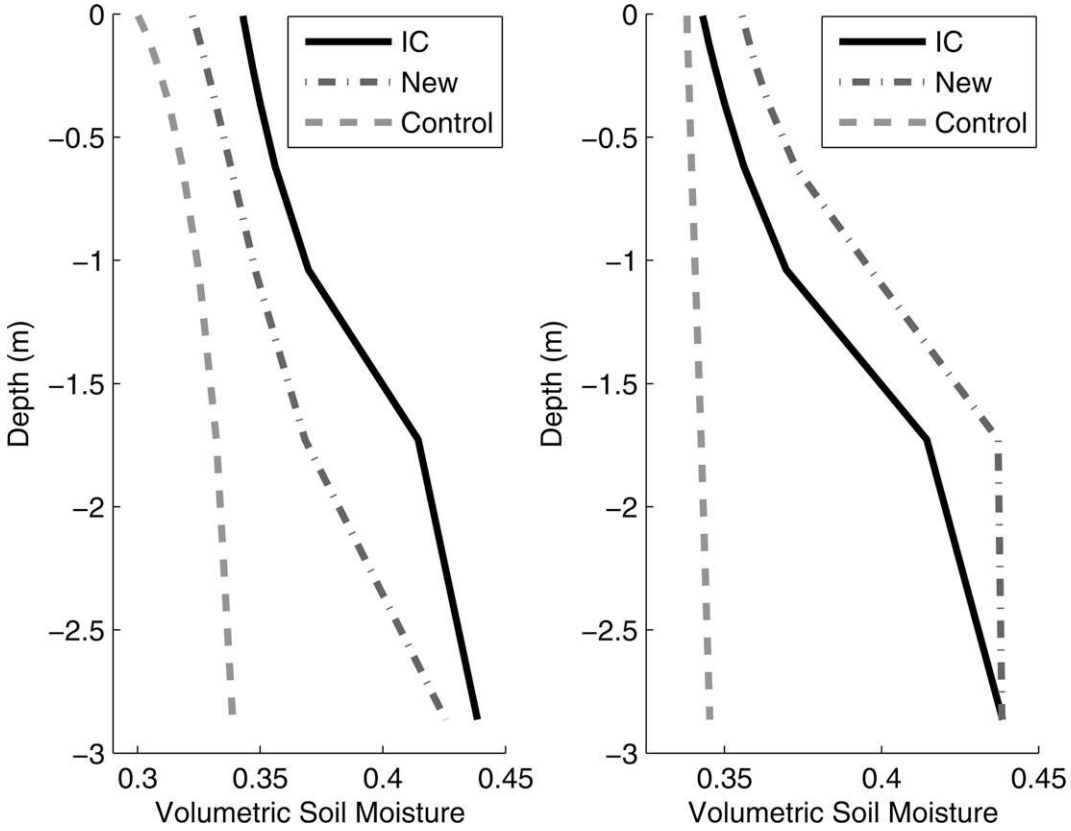

FIG. 6. Soil moisture distribution at the initial equilibrium state with a WTD of 2 m (solid lines) and after 30 days of integrations using (1) and (4) (control simulation, dashed lines) vs (11) and (14) (new simulation, dotted–dashed lines) for (a) $q_0 = -1$ mm day^{-1}, and (b) $q_0 = 1$ mm day^{-1}. The source/sink term is assumed to be zero in (1) and (11).

of integration using (1) and (4) is drier than the initial state, independent of the direction of surface flux. It is particularly surprising that the surface soil moisture is still drier than the initial state for the case of $q_0 = 1$ mm day^{-1} (Fig. 6b). Further analysis indicates that surface soil moisture is—correctly—wetter than the initial state in the first few days (figure not shown). Eventually, the free drainage is too strong and dries up the whole soil column including the top layer (Fig. 6b). At the end of the 30-day integrations using (1) and (4), the water table depths become much deeper than the initial 2 m (4.8 for $q_0 = -1$ and 3.9 m for $q_0 = 1$ mm day^{-1}). In contrast, results using (11) and (14) correctly show the downward propagation of soil moisture anomalies due to the upward or downward surface fluxes (Fig. 6). Accordingly, the water table at the end of the 30-day integrations using (11) and (14) is more reasonable (2.8 for $q_0 = -1$ and 1.5 m for $q_0 = 1$ mm day^{-1}).

The infiltration rate ($q_0 = 1$ mm day^{-1}) in Fig. 6b is small. If q_0 is substantially increased, (14) is effectively equivalent to the zero flux condition, leading to a fully saturated state. In contrast, the free drainage condition (4) will lead to the final state that can be roughly estimated from (10). On the other hand, if bottom drainage is taken as q_0, then $q \equiv q_0$ [or a constant soil water flux in (2)] represents the general steady-state solution of the Richards equation. The constant hydraulic potential in (7) is just a special case—that is, $q_0 = 0$—of this general solution. The question is then, can the numerical solution (6) based on (1) or (11) lead to the correct steady-state solution for $q \equiv q_0 > 0$ from an initially different soil moisture distribution? This would provide more stringent tests than the case with $q_0 = 0$ in Figs. 1–5. Note the steady-state soil moisture profiles with $q \equiv q_0 \neq 0$ have been widely studied in the hydrological community [e.g., based on (2) and with a prescribed water table depth to cover both cases of steady recharge to, and steady capillary rise from, the water table in Salvucci and Entekhabi (1994)]. Here we focus on the solution with the bottom drainage taken as q_0, and the water table depth computed at each time step.

Figure 7 shows the soil moisture distribution after 30 days of integration using (1) or (11) from the initial hydrostatic equilibrium state based on constant hydrau-

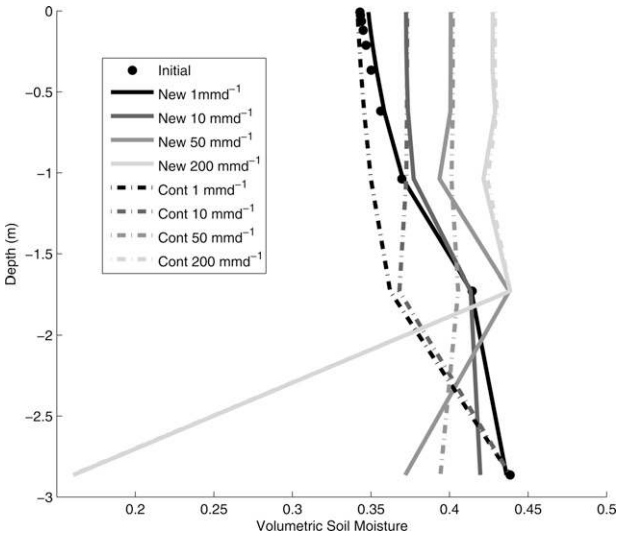

FIG. 7. Soil moisture distribution at the initial state (same as that in Fig. 5) with a WTD of 2 m (dots) and after 30 days of integrations using (1) (control simulation, dotted–dashed lines) and (11) (new simulation, solid lines). The infiltration rate at top and drainage at bottom are the same and taken as 1, 10, 50, and 200 mm day^{-1}, respectively.

lic potential with $z_w = 2$ m. For a small infiltration rate ($q_0 = 1$ mm day^{-1}), the final state using (11) is similar to its initial state, with a slight increase in soil moisture near surface (as a result of infiltration) and a slight decrease in the bottom layer (as a result of drainage). The total soil water is conserved and q is found to be constant (and equal to q_0) at each interface between the soil layers. In other words, (11) leads to the correct equilibrium state for $q_0 = 1$ mm day^{-1}. For $q_0 = 10$ or 50 mm day^{-1}, similar conclusions can be drawn.

When the original Richards equation (1) is used, however, the final state is unrealistic: at $q_0 = 1$ mm day^{-1}, the near-surface soil becomes drier (despite infiltration) and the bottom layer soil becomes wetter (despite drainage). Furthermore, for $q_0 = 1$, 10, or 50 mm day^{-1}, the numerical solution (6) using (1) leads to supersaturated layers with the extra soil water above the saturation removed as runoff. This, in turn, results in the loss of soil water: the total soil water at the end of the 30-day integration using (1) is 1.3084, 1.3379, and 1.3625 m (all less than the initial 1.3728 m) for $q_0 = 1$, 10, or 50 mm day^{-1}, respectively. Note that the significant soil water loss also exists for $q_0 = 0$ in Fig. 2. In contrast, the total soil water does not change with time using (11).

If q_0 is further increased to 200 mm day^{-1}, supersaturated layers would occur using (1) or (11), with significant soil water loss (as runoff) and the total soil water at the end of the 30-day integration is 1.1738 and 1.1715 m, respectively. The overall soil moisture distribution is also similar using (1) or (11) as a result of the strong infiltration (Fig. 7). Furthermore, if the initial soil is very dry (with $z_w = 6$ m), supersaturation does not occur using (1) or (11), and both yield the correct steady state at $q_0 = 1$, 10, 50, or 200 mm day^{-1} (figure not shown). Further tests of (1) and (4) versus (11) and (14) using the full physics in CLM3 over one site will be discussed in section 4, whereas global tests will be discussed in a separate study (DeZe).

Note that although the Clapp–Hornberger formulations in (5) are widely used in land models for weather and climate studies, other formulations are widely used in groundwater hydrology and soil physics studies. The suitability of different formulations or the combination of different formulations for different soil types has been addressed in the past (e.g., Fuentes et al. 1992). The sensitivity of land models to these formulations has also been addressed before (e.g., Shao and Irannejad 1999). As a sensitivity test, we have replaced (5) with the Brooks and Corey (1964) relation and repeated all the simulations and found that our conclusions remain the same. For instance, the comparison of Figs. 3a and 3b indicates that although the exact values of $\theta(z)$ after 30 days of integration depend on the particular relation used, all the points based on Fig. 3a as discussed in section 2d are equally valid for Fig. 3b in which the Brooks and Corey relation is used. The use of the θ-based versus Ψ-based Richards equation will be discussed in section 4.

4. Conclusions and further discussion

The soil moisture (θ)-based Richards equation (1) is widely used to govern the vertical water movement over regions with a deep or shallow water table in land models for weather and climate studies, but its mass-conservative numerical solution (6) is found to be deficient for saturated soil layers in the model domain—that is, with a shallow water table. Furthermore, these deficiencies cannot be reduced by using a smaller grid spacing. The numerical errors are much smaller when the water table is below the model domain. Sensitivity tests in this study demonstrate that these deficiencies are related to the failure of the numerical solution (6) to maintain the hydrostatic equilibrium soil moisture distribution $\theta_E(z)$, which can be derived at each time step from a constant hydraulic—that is, capillary plus gravitational—potential above the water table and represents a steady-state solution of the Richards equation. Therefore, a modified form of the θ-based Richards equation, in which $\Psi[\theta_E(z)]$ is explicitly subtracted at each time step, is developed here to fix these defi-

ciencies. If the same free drainage bottom boundary condition is applied, the use of the original or modified form of the Richards equation does not make much difference, demonstrating the more dominant influence of the bottom boundary condition. This may also explain why the deficiencies of the numerical solution (6) of the θ-based Richards equation (1) were overlooked in the past by the land modeling community, at least for weather and climate studies.

Recognizing the serious deficiencies of the free drainage bottom boundary condition as used by many land models, a new bottom boundary condition (14) based on the hydrostatic equilibrium soil moisture distribution at each time step is also proposed. If the original form of the Richards equation is applied, the new bottom condition can reduce, but cannot remove, the deficiencies of the numerical solution (6) in comparison with the free drainage condition. Using the modified form of the Richards Eq. (11) along with the new bottom condition (14), however, can remove the above deficiencies of the numerical solution (6) with a deep or shallow water table.

These results are based on the expressions in CLM3 for the fluxes in the numerical solution (6). Although we expect that our conclusions should remain the same using expressions in other land models, further studies by different modeling groups are still needed to verify it.

With the central role of θ in land–atmosphere interactions, our modified form of the Richards Eq. (11) along with the new boundary condition (14) is expected to significantly affect the energy, water, and carbon fluxes as well as the dynamic growth of vegetation in land models for weather and climate studies. In particular, (11) and (14) allow the (upward) capillary pump of water from below the model domain to help maintain the transpiration during the dry season (e.g., over the Amazon Basin, Nepstad et al. 1994), which has been a significant issue for many land models (Dickinson et al. 2006). As a preliminary test, we have implemented (11) and (14) in CLM3 (Oleson et al. 2004) and run the model using the atmospheric forcing data for the period of 1970–2004 from Qian et al. (2006). In both simulations, full model physics (e.g., root distribution, surface and subsurface runoff, transpiration and evaporation, and snow) is included. Figure 8 shows that, compared with the control simulation using (1) and (4), the new simulation with (11) and (14) is much closer to the in situ soil moisture observations over Illinois (Hollinger and Isard 1994). Note that there is a low point between 1.5- and 2-m depth—that is, layer 9 in CLM3—because the lateral drainage in CLM3 is assumed to occur in layers 6–9 only, whereas the free drainage occurs in the bottom or layer 10. A more comprehensive evaluation

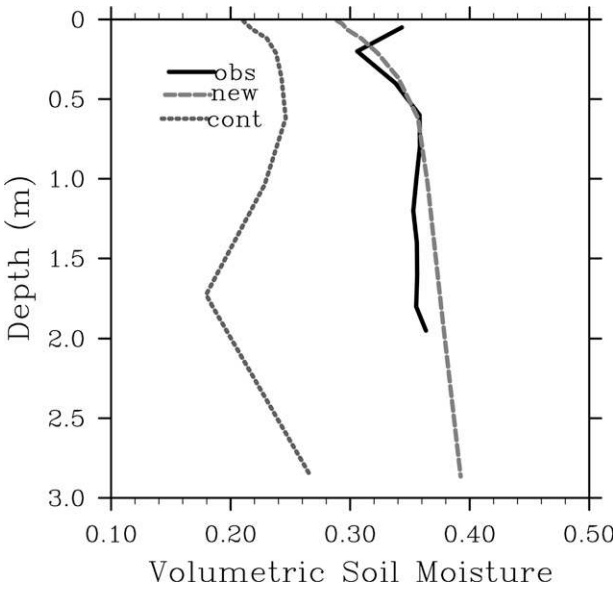

FIG. 8. Vertical profile of the averaged volumetric soil moisture from 1990–2004 for CLM3—that is, with (1) and (4); labeled "cont"—CLM3.0 with the modified form of the Richards equation (11) along with the bottom boundary condition (14) (labeled "new"), and the in situ observations over Illinois (labeled "obs").

of the positive effects of (11) and (14) on the global offline land modeling will be reported in a separate paper (DeZe) that will also include the further improvement of the bottom boundary condition by considering the horizontal movement of soil water.

The Richards equation with Ψ (rather than θ) as the dependent variable is widely used in the studies of groundwater hydrology and soil physics (e.g., Neuman 1973; Milly 1985). For the numerical solution of the Ψ-based Richards equation, subtraction of the equilibrium state is not needed but maintaining the mass balance is challenging (Celia et al. 1990; Pan and Wierenga 1995). For the numerical solution (6) of the θ-based Richards Eq. (1) here, in contrast, mass is conserved but maintaining the equilibrium state is challenging. Note that the removal of supersaturated water as runoff at the end of each time step is not regarded as a violation of the mass conservation in a land model. The mass conservation problem for the Ψ-based equation has been largely fixed through the use of various modified or mixed forms of the equation (Celia et al. 1990; Pan and Wierenga 1995; Ross 2003). Complementary to these efforts, the hydrostatic equilibrium state maintenance problem for the θ-based Eq. (1) is largely fixed here through the use of (11). It will be a future task to compare the accuracy and computational efficiency of the numerical solution (6) using the modified form of the θ-based Richards Eq. (11) versus the numerical solutions of Ψ-based Richards equation (Pan and

Wierenga 1995; Ross 2003) for situations with a deep or shallow water table and with depth-dependent or uniform soil properties.

In the modified form of the Richards equation (11), water table depth is explicitly computed at each time step to obtain the hydrostatic equilibrium soil moisture distribution $\theta_E(z)$. Furthermore, θ in the extra layer below the model domain is directly computed from $\theta_E(z)$. This effectively provides a mechanism for the direct (vertical) coupling of surface and underground water, which is complementary to prior efforts (Liang et al. 2003; Yeh and Eltahir 2005; Maxwell and Miller 2005; Fan et al. 2007). Further discussion of this issue will be provided in DeZe. Significant progress has also been made in recent years in the modeling of horizontal movement of soil water caused by subgrid topography (Koster et al. 2000; Walko et al. 2000; Chen and Kumar 2001; Niu et al. 2005; Yu et al. 2006). With a focus on the vertical θ exchange, our modified form of the Richards equation can also be directly used in combination with these topography-generated runoff formulations. In fact, the horizontal movement of soil water has been included and is needed for global offline simulations in our subsequent study (DeZe). Finally, if a land model contains a river transport submodel (e.g., Oleson et al. 2004), the change in the horizontal water flux can be added to θ in the extra layer, providing a direct coupling mechanism between the horizontal transport of water (between model grids) and the vertical θ exchange within a grid. These issues are all related to (11) and (14) but are also affected by other processes in each land model and hence are better left for future studies using various land models.

Acknowledgments. This work was supported by NSF Grant ATM0634762, NASA Grant NNG06GA24G, and NOAA Grant NA07NES4400002. Two anonymous reviewers and the editor (G. D. Salvucci) are thanked for their helpful comments and suggestions.

REFERENCES

Albertson, J. D., and N. Montaldo, 2003: Temporal dynamics of soil moisture variability: 1. Theoretical basis. *Water Resour. Res.,* **39,** 1274, doi:10.1029/2002WR001616.

Bonan, G. B., and S. Levis, 2006: Evaluating aspects of the community land and atmospheric models (CLM3 and CAM3) using a dynamic global vegetation model. *J. Climate,* **19,** 2290–2301.

Brooks, R.H., and A.T. Corey, 1964: Hydraulic properties of porous media. Hydrology Paper 3, Civil Engineering Department, Colorado State University, 27 pp.

Celia, M. A., E. T. Bouloutas, and R. L. Zarba, 1990: A general mass-conservative numerical solution for the unsaturated flow equation. *Water Resour. Res.,* **26,** 1483–1496.

Chen, J., and P. Kumar, 2001: Topographic influence on the seasonal and interannual variation of water and energy balance of basins in North America. *J. Climate,* **14,** 1989–2014.

Clapp, R. B., and G. M. Hornberger, 1978: Empirical equations for some soil hydraulic properties. *Water Resour. Res.,* **14,** 601–604.

Cosby, B. J., G. M. Hornberger, and T. R. Ginn, 1984: A statistical exploration of the relationships of soil moisture characteristics to the physical properties of soils. *Water Resour. Res.,* **20,** 682–690.

Cox, P. M., R. A. Betts, C. D. Jones, S. A. Spall, and I. J. Totterdell, 2000: Acceleration of global warming due to carbon-cycle feedbacks in a coupled climate model. *Nature,* **408,** 184–187.

Dickinson, R.E., A. Henderson-Sellers, and P.J. Kennedy, 1993: Biosphere–Atmosphere Transfer Scheme (BATS) version 1e as coupled to the NCAR Community Climate Model. NCAR Tech. Note NCAR/TN-387+STR, 72 pp.

——, and Coauthors, 2006: The Community Land Model and its climate statistics as a component of the Community Climate System Model. *J. Climate*, **19,** 2302–2324.

Famiglietti, J. S., and E. F. Wood, 1994: Multiscale modeling of spatially variable water and energy balance processes. *Water Resour. Res.,* **30,** 3061–3078.

Fan, Y., G. Miguez-Macho, C. P. Weaver, R. Walko, and A. Robock, 2007: Incorporating water table dynamics in climate modeling: 1. Water table observations and equilibrium water table simulations. *J. Geophys. Res.,* **112,** D10125, doi:10.1029/2006JD008111.

Fuentes, C., R. Haverkamp, and J.-Y. Parlange, 1992: Parameter constraints on closed-form soil water relationships. *J. Hydrol.,* **134,** 117–142.

Hollinger, S. E., and S. A. Isard, 1994: A soil moisture climatology of Illinois. *J. Climate,* **7,** 822–833.

Holton, J.R., 2004: *An Introduction to Dynamic Meteorology*. 4th ed. International Geophysics Series, Vol. 88, Elsevier, 535 pp.

Koster, R. D., M. J. Suarez, A. Ducharne, M. Stieglitz, and P. Kumar, 2000: A catchment-based approach to modeling land surface processes in a general circulation model. I: Model structure. *J. Geophys. Res.,* **105,** 24 809–24 822.

Liang, X., Z. Xie, and M. Huang, 2003: A new parameterization for surface and groundwater interactions and its impact on water budgets with the variable infiltration capacity (VIC) land surface model. *J. Geophys. Res.,* **108,** 8613, doi:10.1029/2002JD003090.

Lohmann, D., and Coauthors, 1998: The Project for Intercomparison of Land-surface Parameterization Schemes (PILPS) phase 2(c) Red–Arkansas River basin experiment: 3. Spatial and temporal analysis of water fluxes. *Global Planet. Change*, **19,** 161–179.

Maxwell, R. M., and N. L. Miller, 2005: Development of a coupled land surface and groundwater model. *J. Hydrometeor.,* **6,** 233–247.

Milly, P. C. D., 1985: A mass-conservative procedure for time-stepping in models of unsaturated flow. *Adv. Water Resour.,* **8,** 32–36.

Mitchell, K., and Coauthors, 2004: The multi-institution North American Land Data Assimilation System (NLDAS): Utilizing multiple GCIP products and partners in a continental distributed hydrological modeling system. *J. Geophys. Res.*, **109,** D07S90, doi:10.1029/2003JD003823.

Nepstad, D. C., and Coauthors, 1994: The role of deep roots in the hydrological and carbon cycles of Amazonian forests and pastures. *Nature*, **372,** 666–669.

Neuman, S. P., 1973: Saturated-unsaturated seepage by finite elements. *J. Hydraul. Div. Amer. Soc. Civ. Eng.,* **99** (HY12), 2233–2250.

Niu, G.-Y., Z.-L. Yang, R. E. Dickinson, and L. E. Gulden, 2005: A simple TOPMODEL-based runoff parameterization (SIMTOP) for use in global climate models. *J. Geophys. Res.,* **110,** D21106, doi:10.1029/2005JD006111.

Oleson, K. W., and Coauthors, 2004: Technical description of the Community Land Model (CLM). NCAR Tech. Note NCAR/TN-461+STR, 174 pp.

Pan, L., and P. J. Wierenga, 1995: A transformed pressure head-based approach to solve Richards' equation for variably saturated soils. *Water Resour. Res.,* **31,** 925–931.

Qian, T., A. Dai, K. E. Trenberth, and K. W. Oleson, 2006: Simulation of global land surface conditions from 1948–2004. Part I: Forcing data and evaluation. *J. Hydrometeor.,* **7,** 953–975.

Richards, L. A., 1931: Capillary conduction of liquids through porous mediums. *Physics,* **1,** 318–333.

Ross, P. J., 2003: Modeling soil water and solute transport—Fast, simplified numerical solutions. *Agron. J.,* **95,** 1352–1361.

Salvucci, G. D., and D. Entekhabi, 1994: Equivalent steady soil moisture profile and the time compression approximation in water balance modeling. *Water Resour. Res.,* **30,** 2737–2749.

Sellers, P. J., and Coauthors, 1996: A revised land surface parameterization (SiB2) for atmospheric GCMs. Part I: Model formulation. *J. Climate*, **9,** 676–705.

Shao, Y., and P. Irannejad, 1999: On the choice of soil hydraulic models in land-surface schemes. *Bound.-Layer Meteor.,* **90,** 83–115.

Thornton, P. E., and N. E. Zimmermann, 2007: An improved canopy integration scheme for a land surface model with prognostic canopy structure. *J. Climate,* **20,** 3902–3923.

Walko, R. L., and Coauthors, 2000: Coupled atmosphere–biosphere–hydrology models for environmental modeling. *J. Appl. Meteor.*, **39,** 931–944.

Yeh, P. J.-F., and E. A. B. Eltahir, 2005: Representation of water table dynamics in a land surface scheme. Part I: Model development. *J. Climate,* **18,** 1861–1880.

Yu, Z., D. Pollard, and L. Cheng, 2006: On continental-scale hydrologic simulations with a coupled hydrologic model. *J. Hydrol.,* **331,** 110–124.